

DETERMINATION OF HYPOCENTERS AND MAGNITUDES OF LOCAL EARTHQUAKES AROUND COMOROS

Mariama MADI¹
MEE22703

Supervisor: Tatsuhiko HARA^{2*}

ABSTRACT

We have conducted hypocenter determinations and calculated local magnitudes for five events, which occurred on November 23, 24, and 29, 2019, May 29, 2020, and October 13, 2022, around Comoro Islands. We retrieved data recorded by the local seismic network and picked P and S arrival times using the seismograms and the probability density functions of their amplitudes. We determined hypocenters using two velocity models, which are a global model and a local model, respectively. The focal depth was set to 10 km considering the difficulty in its determination. The RMS (root-mean-square) residuals for the local model are found to be smaller, which implies that the local model is more appropriate. Then we calculated local magnitudes by amplitude measurements of synthetic Wood-Anderson seismograms. Since duration magnitude is the only one calculated at the Karthala Volcano Observatory of Comoros, the local magnitude will be the second magnitude to be registered in the observatory bulletin. Although the calculated local magnitudes are comparable to the duration magnitudes, their correlation is unclear. Further analyses are necessary to establish their relation. The methods and analyses used in this study are likely to improve earthquake monitoring at the Karthala Volcano Observatory of the Comoros. Further analyses using a larger dataset will be useful for monitoring the seismic and volcanic activities in the study region.

Keywords: Hypocenter, Local magnitude, Comoro Islands

1. INTRODUCTION

The Comoro Islands is a chain of four islands located in the entry of the Mozambique Channel between the southeastern part of Africa and the northwestern side of Madagascar. The magmatism and morphology of the islands are comparable to those of the volcanism of the Hawaiian Islands which are known to have various of stages and erosion development processes. The Comoros hotspot is one of the hotspot volcanoes: (e.g., Steinberger, 2000). The Comoro Islands have significant records of basalts and associated volcanic and plutonic rocks that compose them (e.g., Thompson & Flower, 1971; Flower, 1971, 1972, 1973a,b; Ludden, 1977), while the islands become younger toward the Western side.

The Gde-Comore-Island is younger than the other three archipelago islands, Moheli, Anjouan, and Mayotte. The active Karthala volcano induces seismic activities recorded in the Gde-Comore Island. The volcanic activities in 2004, 2005 (Thivet et al., 2022), 2006 (Morin, et al., 2009), 2007 (<https://doi.org/10.5479/si.GVP.BGVN200701-233010>), and the recent 2022 volcano-seismic activity

¹ National Data Center (NDC) and Karthala Volcano Observatory (OVK), under the National Center of Documentation and Scientific Research (CNDRS), Moroni, Comoros.

² Professor, International Institute of Seismology and Earthquake Engineering, Building Research Institute.

* Chief examiner

require more attention in terms of volcano monitoring. The improvement of the volcano earthquake observation capacity is crucial for the Gde-Comore-Island. In this work, we analyzed the local network data applying the new method using the PDF (Probability Density Function) of seismic wave amplitudes Oshima and Takenaka (2020, 2022) to pick P and S arrivals. Using HYPOCENTER software program (Lienert et al., 1986; Lienert & Havskov, 1995) installed in SEISAN Software (Havskov & Ottemoller, 1999; Havskov et al., 2020), we determined the hypocenters of five local events, that is, three events in 2019 (May 23, 2019, May 24, 2019, and May 29, 2019), one in 2020 (November 24) and one in 2022 (October 13) around the island and with six stations from the local network. We calculate the local magnitudes using the SEISAN software and compare them to the duration magnitudes obtained from the volcano observatory bulletin, which are determined routinely.

2. METHODOLOGY

This chapter explains the methods of picking the P and S arrivals, hypocenter determination, and local magnitude calculation.

2.1. Phase picking using the probability density function of seismic waveform amplitudes

Oshima and Takenaka (2020) developed a method for picking the P and S arrivals based on the probability density function (PDF) of the seismic wave amplitudes. Oshima and Takenaka (2022) developed a new method for enhancing direct waves using the PDF of waveform amplitude. The KLD (Kullback and Leibler, 1951) is used to quantify the dissimilarity between the PDF and the Gaussian or Rayleigh distribution.

$$K_{LD}(p, q) = \int_{-\infty}^{\infty} p(x) \log \frac{p(x)}{q(x)} dx, \quad (1)$$

where, $p(x)$ and $q(x)$ are the PDFs, and the similarity between $p(x)$ and $q(x)$ is quantified. Oshima and Takenaka (2022) calculated the KLD between the PDF of the absolute amplitude and its corresponding Rayleigh distribution as follows:

$$K_{LD}(p, q) = \sum_{i=1}^{nbin} p(x_i) \log \frac{p(x_i)}{q(x_i)}, \quad (2)$$

where, $nbin$ is the number of bin, which is \sqrt{nwind} ; $nwind$ is the number of the normalized absolute amplitude data, $x(k)$ ($k = 0, 1, \dots, nwind - 1$); x_i is the central value of the i -th bin; $p(x_i)$ is the number of the data in the i -th bin divided by $nwind$; and $q(x_i)$ is the value of the Rayleigh distribution. The baseline is corrected before calculations. The Rayleigh distribution is represented by

$$R(x) = \frac{x}{\sigma^2} \exp\left(-\frac{x^2}{2\sigma^2}\right), \quad (3)$$

and the parameter σ is calculated as

$$\sigma = \sqrt{\sum_{k=1}^{nwind} \{x(k)\}^2 / 2nwind}, \quad (4)$$

Oshima and Takenaka (2020) used the two KLD indexes. The first index is KLD1 defined as the KLD between the PDF of the observed amplitude waveform, and the Raleigh or Gaussian distribution. In this study, we used the Rayleigh distribution following Oshima and Takenaka (2022). The second index is KLD2 defined as the KLD between the PDFs for the adjacent time windows on a single seismic trace. They used KLD1 for the P-phase picking on the amplitude of the vertical component. Both KLD1 and KLD2 are used for S-phase picking. Although Oshima and Takenaka (2020) showed that this technique was applicable to automatic phase picking, we used these KLDs to support manual picking.

2.2. Hypocenter Determination

We used the HYPOCENTER software program (Lienert et al., 1986; Lienert & Havskov, 1995) to determine the hypocenters using the P and S arrival times from the local data. It is included in the SEISAN software (Havskov & Ottemoller, 1999; Havskov et al., 2020), which can be used for

earthquake data analyses at seismic observations. HYPOCENTER is a default program for hypocenter determination in the SEISAN, for which a file including information such as station locations and velocity models should be prepared before analyses.

2.2.1. Velocity Models

We used the two velocity models to determine the hypocenters using HYPOCENTER: the iasp91 model (Kennett and, Engdahl, 1991) and a model set at -11.5° Latitude and 43.5° Longitude in CRUST 1.0 (Laske, et al., 2013). We used “Crust 1.0 and Google Earth” (<https://github.com/jrleeman/Crust1.0>) to extract the model parameters of CRUST1.0. For the latter, we applied the model parameters in the crust and upper mantle and refer to the model as CR1. Table 1 shows CR1 model. The thickness of iasp91model is 35 km, while for CR1 it is thinner (14.15 km). Model CR1 includes a thin relatively slow velocity layer at the top.

Table 1. The Model parameters of the model from CRUST 1.0 (Laske, et al., 2013), which we refer to as the CR1 model.

Depth (km) to the top of the layer	Vp (km)	Vs (km)
0	5	2.7
1.41	6.5	3.7
4.24	7.1	4.05
14.15	8.13	4.51

2.3. Local Magnitude Calculation

We used SEISAN to measure the amplitudes and calculate the local magnitudes. The Synthetic Wood-Anderson seismograms are calculated by deconvolution using the instrumental responses and the convolution of the Wood-Anderson seismograph response. Following Havskov and Ottemoller (2010), we used vertical component seismograms and applied a high-band pass filter in cases where the seismic signals are difficult to see on the synthetic Wood-Anderson seismograms. In SEISAN, the effect of the high-band pass filter is corrected for amplitude measurements. The local magnitude (ML) is calculated by the following formular (Borman et al 2013; Borman and Dewey, 2014):

$$ML = \log_{10}(A) + 1.11 \log_{10}R + 0.00189 * R - 2.9, \quad (5)$$

where, A is the maximum amplitude (nm) of the synthetic Wood-Anderson seismogram, and R is the hypocentral distance (km). The coefficients for the first and second terms are from Hutton and Boore (1987), who obtained their local magnitude formula for Southern California.

3. DATA AND PROCESSING PROCEDURE

3.1. Data and Seismic Network

We analyzed five earthquakes that occurred around Comoros Islands. We selected them by considering the data availability and their relatively large sizes compared to events in the main island. As mentioned in the Introduction section, the Karthala Volcano Observatory of Comoros routinely determines the duration magnitudes using Seiscomp3 (Helmholtz Centre Potsdam GFZ German Research Centre for Geosciences and gempa GmbH, 2008). We retrieved the waveform data recorded at six stations (CAB, DEMB, GRIL, MOIN, NBC, NTC) of the Karthala Volcano Observatory of Comoros.

3.2. Procedure of Data Processing

3.2.1. Picking of P and S Arrival Times

Figure 1 shows examples of the SAC data and KLD1 and KLD2 results. The event occurred on November 24, 2020, and the station is DEMB. We used 2s time window for the KLD1 calculation and 2s and 4s as time windows for the KLD2 calculation. The first to third traces from the top show the original three-component waveforms; the fourth to sixth traces from the top show their KLD1 waveforms; The seventh to ninth traces from the top denotes the KLD2 waveforms for with a is 2 s time window; and the 10th to 12th traces from the top display the KLD2 waveforms with a 4s time window. The arrivals of P and S waves can be seen on the KLD seismograms. In some cases, P and S arrivals are not clear on KLD seismograms.

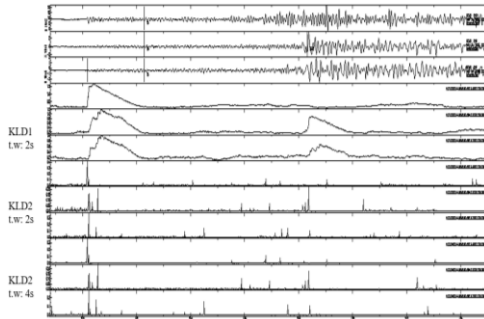


Figure 1. Example of the SAC waveform data, and their KLD1 and KLD2. The event is the one that occurred on November 24, 2020, and the station is DEMB.

We calculated KLDs by the procedures explained in 2.1. As Oshima and Takenaka (2020) showed if the coda part is used for the Rayleigh distribution the changes of KLD1 will be larger. Also it is desirable to further examine the effects of time widows and noise levels. The application of band-pass filtering will be another subject to be studied in future.

3.2.2. Hypocenter Determination

After picking the P and S arrival times, we put the arrival time data in the SEISAN database and conducted hypocenter determination using HYPOCENTER. The station locations are put in STATIONX.HYP, which is used by HYPOCENTER. We prepared this file for model iasp91 and CR1, respectively. The waveform data, which were converted to miniSEED format, were registered in the SEISAN database. We tried to determine the origin time and the hypocenter, however found that it was difficult to determine focal depths due to the limited number of data. Therefore, we decided to fix the focal depth for each event and set it to 10 km in this study.

3.2.3. Amplitude measurement

After conducting the hypocenter determinations, we proceeded with the amplitude measurements using the vertical component seismograms. We used the SEISAN software (Havskov & Ottemoller, 1999; Havskov et al., 2020) to calculate the synthetic Wood-Anderson seismograms and used them for manual measurements after applying high band pass filter (15-25HZ). As stated in section 2.3, the effect of the high-band pass filter is corrected in SEISAN.

4. RESULTS AND DISCUSSION

4.1. Hypocenter Determination

We determined hypocenters for the five events presented in Table 2 using the method and procedure explained in the previous chapters. Figures 2(a) and (b) show the results of these calculations. The errors of the origin times and epicenters for model CR1 are smaller than or comparable to those for model iasp91 (Kennett and Engdahl, 1991). The RMSs for model CR1 are smaller than those for model iasp91. These imply that CR1 is better than iasp91 for hypocenter determination for events in the study region. Since the number of the analyzed events are small, further investigations are necessary to find a suitable model. The focal depths of some hypocenters in the bulletin of the Volcano Observatory are very deep, say around 50 km or larger than 100 km. Considering the tectonic environment of the study area, such deep events are not likely, and probably they are due to the difficulty to determine focal depths. Therefore for such a case, it is better and reasonable to set a shallow focal depth.

Table 2. Hypocenters determined using the CR1 and iasp91 (Kennett and Engdahl, 1991) models for the five events.

Event	Velocity model	Date	Origin time	Time error	Latitude	Lat.error	Longitude	Lon.error	RMS
1	crust1.0	2019 May 23	22.23.57.5	0.530	-12.096	14.7	42.394	6.6	0.23
	iasp91	2019 May 23	22.23.55.4	0.660	-12.222	12.1	42.562	7.5	0.48
2	crust1.0	2019 May 24	02.17.46.0	0.600	-12.688	31.4	41.647	16.9	0.3
	iasp91	2019 May 24	02.17.45.1	0.610	-12.579	26	41.939	15	0.48
3	crust1.0	2019 May 29	17.49.48.4	0.330	-12.111	5.6	43.911	3.8	0.11
	iasp91	2019 May 29	17.49.47.8	1.17	-12.04	13.3	43.859	10.2	0.58
4	crust1.0	2020 Nov 24	23.45.16.0	0.290	-12.485	3	43.188	8	0.07
	iasp91	2020 Nov 24	23.45.13.6	1.73	-12.33	15.5	42.947	22.2	1.15
5	crust1.0	2022 Oct 13	10.11.24.7	0.850	-12.274	14.8	44.241	11.3	0.4
	iasp91	2022 Oct 13	10.11.23.3	1.21	-12.05	14	44.188	9.4	0.62

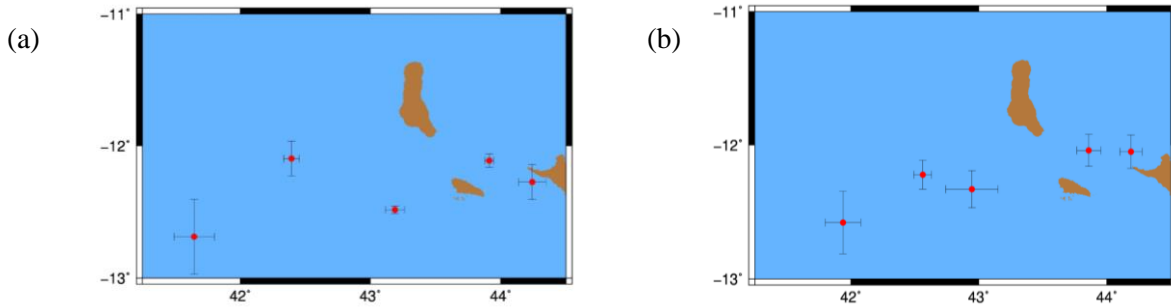


Figure 2. (a) the epicenters determined using the CR1 model. (b) the epicenters determined using iasp91 model (Kennett & Engdahl, 1991). The focal depths are fixed to 10km.

4.2. Local magnitude calculation

We calculated ML for the five events using the hypocenters obtained for CR1 model. Figure 3 shows the comparison between ML and Md calculated by the Karthala Volcano Observatory of the Gde-Comore Island. The estimates themselves for ML are comparable to those of Md. Also, the estimates of Md are larger than those of ML for all the events. Considering the difficulty associated with amplitude measurements for small events, it is necessary to calculate Md and register it into the earthquake bulletin continuously. Further local magnitude analyses of more events are necessary to evaluate the accuracy of Md and the relation between Md and ML.

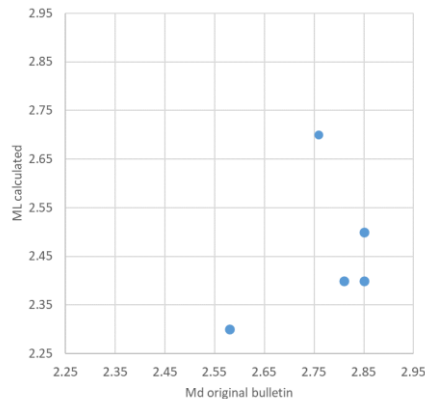


Figure 3. Comparison between ML calculated in this study and Md from the observatory bulletin.

5. CONCLUSIONS

In this study, we determined hypocenters and calculated local magnitudes for five earthquakes, that occurred in 2019, 2020, and 2022, using waveform data recorded at the stations of the Karthala Volcano

Observatory. First, we picked P and S arrival times using the recorded seismograms and their KLD seismograms, which were calculated following the methods of Oshima and Takenaka (2020, 2022). Then we determined hypocenters using HYPOCENTER program in SEISAN software, in the database of which P and S arrival times waveforms are put. We used two velocity models for our hypocenter determination, which are CR1 from CRUST 1.0 (Laske et al., 2013) and iasp91 (Kennett and Engdahl, 1991). We fixed the focal depths at 10km for all the five events. The small RMS residuals imply model CR1 is better for hypocenter determination.

We measured amplitudes of synthetic Wood-Anderson seismograms calculated for the observed seismograms using SEISAN. We then calculated ML using the measured amplitudes and the hypocenter distances from the hypocenters obtained for model CR1; we used the formula of the IASPEI standard procedure with the coefficients for southern California based on the work of Hutton & Boore (1987). The calculated ML estimates are comparable to those of Md calculated in the Observatory bulletin. It seems that the correlation between them is not clear. However, the number of events needs to be increased to evaluate their relation more precisely.

ACKNOWLEDGEMENTS

I would like to take this opportunity to express my sincere gratitude to Dr. Tatsuhiko Hara for supervising me during my study and providing me with adequate guidance.

REFERENCES

- Bormann, P., & Dewey, J. W. (2014). IS3. 3. NMSOP2. German Research Centre for Geosciences.
- Bormann, P., Wendt, S., & DiGiacomo, D. (2013). In New manual of seismological observatory practice 2 (NMSOP2) (pp. 1-259). Deutsches GeoForschungsZentrum GFZ.
- Flower, M. (1971). *Contributions to Mineralogy and Petrology*, 31(4), 335-346.
- Flower, M. (1972). *Bulletin Volcanologique*, 36, 238-250.
- Flower, M. (1973a). *Chemical Geology*, 12(2), 81-98.
- Flower, M. (1973b). *Contributions to Mineralogy and Petrology*, 38(3), 237-260.
- Global Volcanism Program. (2007). *Bulletin of the Global Volcanism Network*, 32:1. Smithsonian Institution. <https://doi.org/10.5479/si.GVP.BGVN200701-233010>
- Havskov, J., Voss, P. H., & Ottemöller, L. (2020). *Seismological Research Letters*, 91(3), 1846-1852.
- Havskov, J., & Ottemoller, L. (1999). *Seismol. Res. Lett*, 70(5), 532-534.
- Helmholtz Centre Potsdam GFZ German Research Centre for Geosciences and gempa GmbH (2008). GFZ Data Services. doi:10.5880/GFZ.2.4.2020.003.
- Hutton, L. K., & Boore, D. M. (1987). *Bulletin of the SSA*, 77(6), 2074-2094.
- Kennett, B., & Engdahl, E. (1991). *Geophysical Journal International*, 105(2), 429-465.
- Kullback, S., & Leibler, R. A. (1951). *The annals of mathematical statistics*, 22(1), 79-86.
- Laske, G., Masters, G., Ma, Z. & Pasyanos, M. (2013). Abstracts, 15, Abstract EGU2013-2658.
- Lienert, B. R., Berg, E., & Frazer, L. N. (1986). HYPOCENTER: *Bulletin of the Seismological Society of America*, 76(3), 771-783.
- Lienert, B. R., & Havskov, J. (1995). *Seismological Research Letters*, 66(5), 26-36.
- Ludden, J. (1977). *Contributions to Mineralogy and Petrology*, 64(1), 91-107.
- Morin, J., Lavigne, F., Bachelery, P., Finizola, A. and Villeneuve, N., 2009. *Shima: The International Journal of Research into Island Cultures.*, 3(1), pp.33-53.
- Oshima, M., & Takenaka, H. (2020). *Bulletin of the Seismological Society of America*, 110(2), 763-782.
- Oshima, M., & Takenaka, H. (2022). *Geophysical Journal International*, 231(1), 327-354.
- Steinberger, B. (2000). *Journal of Geophysical Research: Solid Earth*, 105(B5), 11127-11152.
- Thivet, S., Carlier, J., Gurioli, L., Di Muro, A., Besson, P., Smietana, M., . . . Nedelec, J.-M. (2022). *Journal of Volcanology and Geothermal Research*, 424, 107500.
- Thompson, R., & Flower, M. (1971). *Earth and Planetary Science Letters*, 12(1), 97-107.